

Large interfacial exchange fields in a thick superconducting film coupled to a spin filter tunnel barrier

Avradeep Pal* and M. G. Blamire

Department of Materials Science, University of Cambridge, 27 Charles Babbage Road, Cambridge CB3 0FS, UK

The differential conductance of NbN/GdN/TiN superconductor / ferromagnetic insulator / normal metal junctions, with a thick NbN layer shows a large zero-field voltage offset interpreted as a spin-filtered Zeeman splitting of the NbN density of states (DOS) by an effective exchange field (H_0) from the GdN. The splitting increases linearly with applied field (H_{ext}) enabling the relative sign of H_0 and H_{ext} to be determined. We show that the short NbN coherence length concentrates H_0 at the NbN/GdN interface and eliminates any averaging over the GdN domain structure leading to a large zero-field splitting.

PACS: 74.45.+c, 73.40.Gk, 72.25.-b

In an external magnetic field H_{ext} , the quasiparticle density of states (QP-DOS) of a superconductor (S) undergoes Zeeman splitting such that spin-up, down states are changed in energy by $E_Z = \pm \mu_B \mu_0 H_{ext}$, where μ_0 is the vacuum permeability, and μ_B is the Bohr magneton. The spin splitting of the tunnel conductance spectrum (see Fig. 1(a)) which arises from this was originally observed in Al/Al₂O₃/Ag superconductor-insulator-normal metal (S/I/N) tunnel junctions by Meservey *et al.* [1] and developed into a technique by which the spin polarization p of a ferromagnet (F) counterelectrode can be determined by fitting the tunnel conductance arising from the sum of p -weighted Zeeman split QP-DOS [2].

The proximity effect between a conventional s-wave S and a metallic F is controlled by the Fulde-Ferrell-Larkin-Ovchinnikov (FFLO) theory [3,4], where electron pairing derived from S can co-exist with the exchange fields of the F. The inverse proximity effect, the existence of magnetic order in S, also occurs [5] but has so far only been observed indirectly [6]. In contrast, the *primary* interaction between a superconductor and a ferromagnetic insulator (S/FI) is an inverse proximity effect in which the superconductor experiences an effective intrinsic internal exchange field (H_0) predicted by de Gennes [7] to be inversely proportional to the thickness of the S layer (l_S) in the limit where l_S is much less than the superconducting coherence length (ξ_S). The existence of this exchange field has been proved by experiments in which ultra-thin Al S films were proximity coupled to FI europium chalcogenides EuO [8] and EuS [9-11] in which Zeeman splitting of the QP-DOS was observed.

Figure 1(a) illustrates the general Meservey-Tedrow [1] behavior of an S/I/N junction in the presence of a magnetic field or an exchange field arising from contact with an FI layer located below the S layer, which does not participate in the transport process as in experiments discussed earlier [8,11]. Here, four prominent features corresponding to the alignment of the spin-up and spin-down S gap edges with the Fermi energy of the N layer would be observed in the tunneling conductance curves as the QP-DOS peaks align with the N Fermi energy. However, since we use a 3 nm

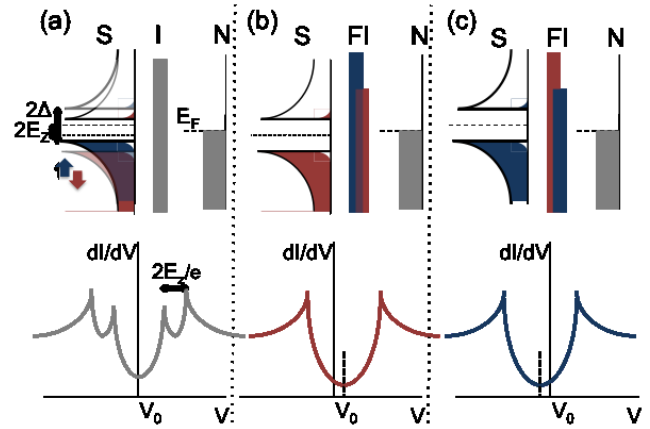


FIG 1 (Color online) Upper row: diagrams representing the participating DOS during transport process in 3 different instances: (a) exchange split S layer and non-magnetic insulating layer, (b) exchange split S layer and an ferromagnetic insulator with down spins as major spin channel, (c) exchange split S layer and an FI layer with up spins as major spin channel. Lower row: corresponding conductance spectra for the three cases.

GdN layer as the spin-filtering FI barrier [12], which is known to induce approximately 95% spin polarization (P) at 4 K [13], the tunneling conductance spectra will effectively carry information of only one spin band of the quasiparticle density of states (DOS) of the NbN layer (Fig. 1(b,c)) and so the conductance spectrum should be that of a conventional S/I/N device with a voltage offset (V_0) equal to the Zeeman energy. As illustrated in Fig. 1(b,c) reversing the magnetization direction of the FI reverses the voltage offset.

In fact, Zeeman splitting of the QP-DOS has so far only been observed in Al; in this Letter, we report results of experiments performed on NbN(100)/GdN(3)/TiN(30) S/FI/N tunnel junctions where the TiN is non-superconducting under the growth conditions used here and the brackets contain the layer thickness in nm. Since $\xi_{NbN} \sim 5$ nm, $l_{NbN} \gg \xi_S$ and so these experiments are in the opposite limit to previous studies in which $l_S \ll \xi_S$; the tunneling conductance spectra therefore reflect the

exchange splitting precisely at the S/FI interface rather than that averaged over the entire superconductor thickness [7].

Trilayer films were grown on oxidized Si substrates pre-coated with a 10 nm layer of MgO; the MgO layer helps to protect the oxidized Si during fabrication by acting as an etch stop layer. We used reactive dc sputtering in an Ar/N₂ atmosphere from Nb and Gd and Ti metal targets in an ultra-high vacuum chamber without breaking the vacuum. Mesa-type square $7 \times 7 \mu\text{m}^2$ tunnel junctions were fabricated using a four-stage lithography process similar to the process described elsewhere [14]. The only difference in the process steps was that the top TiN layer could not be etched by a CF₄ plasma, and hence controlled Argon ion milling had to be performed. Fabricated junctions were then measured by a four-point technique using a closed-cycle measurement system at 3.2K.

Using our standard procedure for calculating the spin polarization at low temperatures from the RT curve [13], we estimate a spin polarization of approximately 97% at 3 K for the GdN tunnel barriers reported in this Letter. Figure 2 shows a typical tunnel conductance spectrum of such a S/FI/N junction. The sub-gap conductance spectrum is a V-type shape, instead of the expected U-type arising from a conventional BCS DOS. This is evidence for the smearing of the interfacial DOS [15] due to presence of the magnetic barrier as discussed later. For thinner GdN thicknesses which have a lower barrier magnetism and spin polarization [13] the tunneling spectra assume an increasingly U-type shape, closer to conventional S/I/N behavior associated with non-magnetic insulator (I) barriers.

We observe that the conductance minimum, which in conventional S/I/N junctions should occur at zero bias, is clearly shifted towards positive bias in our junctions. In the absence of any externally applied magnetic field we can assume that the magnitude of offset of the conductance minimum (V_0), is equivalent to the Zeeman splitting arising from the exchange field (H_0) induced in superconducting NbN due to the proximity coupled GdN (see Fig. 1(b)).

$$eV_0 = \mu_B \mu_0 H_0 \quad (1)$$

where e is the electronic charge. V_0 is determined by means of fitting a parabola to the low bias region as shown in left bottom inset to Fig. 2. For the junction in consideration, $V_0 = 0.1 \pm 0.03 \text{ mV}$, and hence using eq. (1), the intrinsic exchange field $\mu_0 H_0 = 1.7 \pm 0.5 \text{ T}$. This is comparable to the saturated exchange fields in EuO/Al and EuS/Al structures [8,11].

The large parallel to the plane critical field of NbN (in excess of 20T) [16] and relatively high gap voltage (V_g for NbN $\sim 2.5 \text{ mV}$) when compared to Al which results in a large paramagnetic (Chandrasekhar-Clogston) limit [17,18] enables us to apply large H_{ext} to our devices and so extend the study to the well-known Meservey-Tedrow type

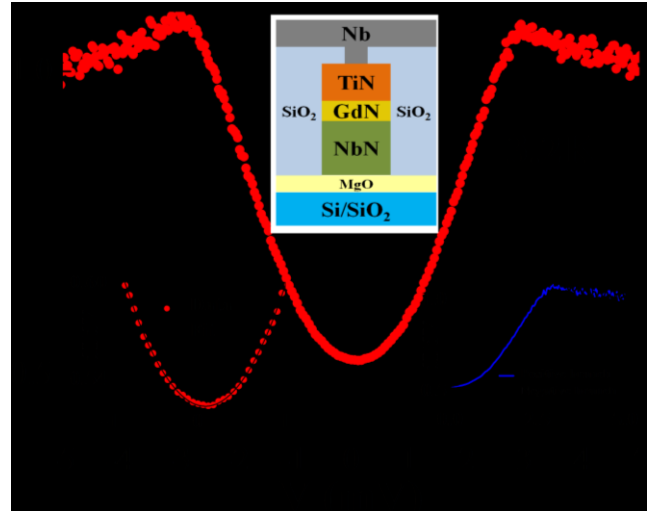


FIG 2. (Color online) Normalized tunneling conductance spectra of a 3nm GdN S/FI/N junction measured at 3.2K. Bottom left inset shows magnified view of the low bias conductance indicating a zero offset of the lowest point in conductance. Bottom right inset is a superposition of the negative voltage branch on the positive one, in order to highlight that even in the absence of any applied magnetic field; there exists an asymmetry throughout the entire voltage range. In both the left and bottom right insets, the x axis represents voltage in mV. Central inset shows a schematic cross section of the side view of the device area.

observations of magnetic field splitting of quasiparticle DOS [1]. However, because the minority spin channel is blocked, on increasing the externally applied magnetic field, instead of observing greater splitting of spin quasiparticle DOS, we should observe a linear shift of the tunneling conductance curve along the voltage axis

The result of applying magnetic fields to the junction is shown in Fig. 3. The error bars are calculated from the errors in the parabolic fit to the low bias region. It can be seen that, although V_0 increases with increasing magnetic field in accordance with eq. (1), the sign of the shift is independent of field direction. The reason for this is explained in the cartoon diagrams in Fig. 3: on reversal of the direction of H_{ext} , the barrier (which is magnetically soft [12]) reverses and so H_0 necessarily reverses with H_{ext} and hence the Zeeman splitting of S is reversed. However, the reversal of the barrier also reverses the spin filter direction and so there should be no detectable change observed in the measured tunneling conductance on reversing the field as illustrated in the right bottom inset to Fig. 3. If we make the reasonable assumption that the exchange field is parallel to the GdN magnetization then eq. (1) can be generalized for the presence of external fields as

$$eV_0 = \mu_B \mu_0 (|H_0| + |H_{ext}|) \quad (2)$$

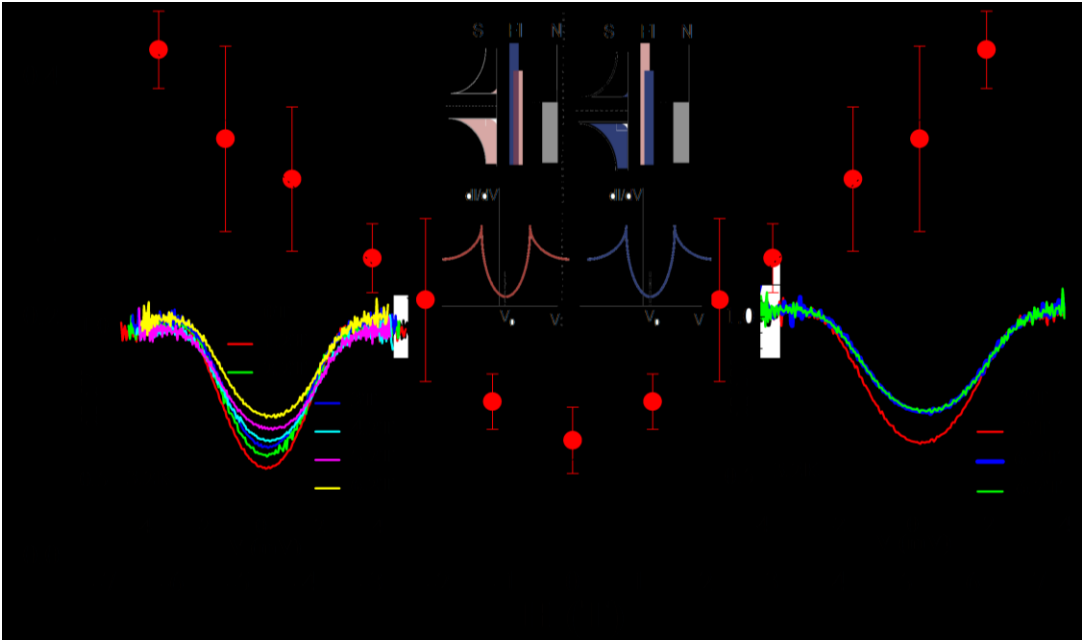


Figure 3 - FIG 3 (Color online) Position of conductance minimum V_0 after applying in plane magnetic fields. Left bottom inset shows the conductance spectra for various values of positive magnetic fields. Right bottom inset shows the conductance spectra for positive and negative fields of identical magnitude. The cartoon diagrams are illustrations of the transport process and spin dependent DOS in negative and positive magnetic fields.

We have fitted Eq. (2) to the data in Fig. 3 as shown with H_0 as the adjustable parameter. Not only does the excellent fit confirm the theoretical understanding, but it provides an improved estimate of the magnitude of $\mu_0 H_0$ as $1.4 \pm 0.15 T$, in the NbN layer

The above results and analysis therefore unambiguously establish the presence of an internal exchange field in the NbN layer. The most striking feature of these results is that the exchange field is easily measurable and comparable to that previously observed in ultra-thin Al [8,9] even though $l_{NbN} \gg \xi_{NbN}$.

In the original theory of the exchange field [7], the exchange coupling between the conduction electrons and the surface spins of the FI is averaged over l_s . By analogy with conventional proximity effect we can replace the average over l_s by one over ξ_S - i.e. the pairing length in contact with the FI. This makes the expression for H_0

$$H_0 = JS(a/\mu_0\mu_B\xi_S) \quad (3)$$

where a is the S lattice parameter and is 0.44 nm for NbN. J has not been estimated for GdN, and so we take the value of $2JS = 100$ meV used by Tedrow *et al* [8] for EuO which is based on an internal exchange splitting of 390 meV [19] and scale this using the measured exchange splitting for 3 nm GdN of 35 meV [12]. Using these values we obtain a value of ~ 6 T for $\mu_0 H_0$ which seems not unreasonable given the uncertainties in many of the parameters and is in any case much closer to the experimental value than is the case for Al/EuO [8].

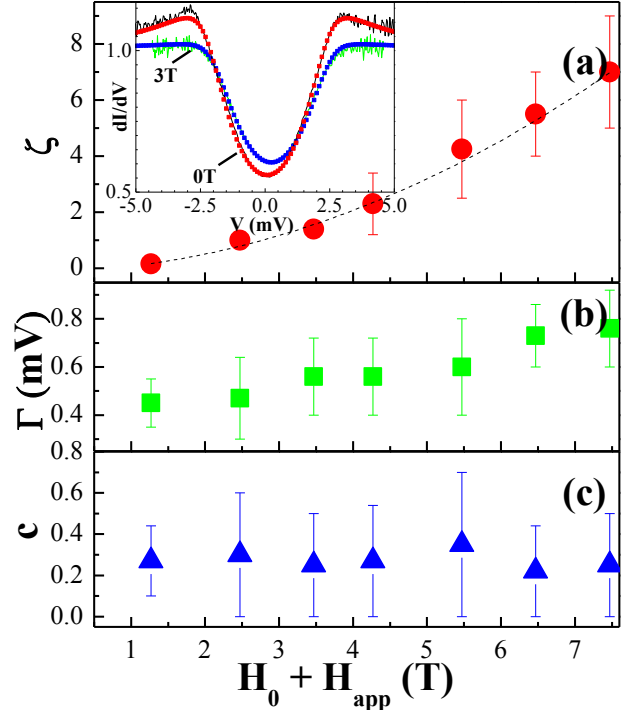


FIG 4. (Color online) Magnetic field dependence of fitting parameters: (a) orbital de-pairing parameter (ζ), (b) Dynes parameter (Γ) and (c) Background DOS (c). Inset to a) are examples of fitted curves at 2 different values of externally applied magnetic fields 0T ($\zeta = 0.2, \Gamma = 0.47$ meV, $c = 0.25$) and 3T ($\zeta = 2.45, \Gamma = 0.55$ meV, $c = 0.25$). Dotted points in inset represent fits to data (solid line). Dotted line in a) is a parabolic fit to the data points.

A key difference between the behavior of NbN/GdN and Al/EuS or Al/EuO is that the latter systems show a zero or greatly suppressed exchange field for $H_{ext} = 0$, which increases rapidly on applying an external field [10,20] whereas the value we measure is, via the fit shown in Fig. 3, independent of field. The low zero-field value of H_0 is explained in ref. [10] as a consequence of averaging over EuS domains with different exchange field directions over $\xi_{Al} = 1600\text{nm}$, although the data of Xiong *et al.* [20] may not be compatible with this explanation. In our case, although there have been no measurements of the GdN domain size in thin films, it is unlikely to be significantly smaller than to ξ_{NbN} and so the averaging over adjacent barrier domains is minimal and so this may explain the difference between the two materials systems.

The main reason for using ultra-thin Al is to minimize spin-orbit effects [1]. At first sight using much thicker films containing NbN which is known to have a significant spin-orbit interaction might be expected to smear the data to a point at which the exchange field could not be accurately measured. In order to investigate the smearing effects in our devices, in Fig. 4, we show fits to experimental data at zero and finite values of H_{ext} . These fits were obtained following the method described in [21] by numerically integrating the tunneling integral for a S/I/N junction assuming that the DOS of the S layer is modified by the presence of an orbital de-pairing parameter (ζ) and a Dynes lifetime broadening parameter Γ [15] and an energy-independent background QP-DOS (c):

$$N(\omega) = \frac{N(0)}{(1+c)} \left\{ \text{Re} \left[\frac{v}{(v^2 - 1)^{1/2}} \right] + c \right\} \quad (3)$$

where $v = u - i\Gamma / \Delta$ and u by $\omega / \Delta = u \left[1 - \zeta / (u^2 - 1)^{1/2} \right]$.

The assumed energy gap $\Delta = 2.2$ mV and we kept this constant for all values of applied field. Using these three parameters is sufficient to phenomenologically capture the broadening due to spin-orbit effects and produce good fits to the experimental data. ζ is found to have a quadratic dependence on the magnetic field as predicted theoretically [22]. Γ increases weakly with magnetic field similar to previous observations [25] but is relatively high; as argued by Dynes *et al.* [15], this is expected for strong-coupling superconductors such as NbN. A previous study has also indicated high values of Γ for bare films of NbN [23].

Although Γ itself accounts for the presence of background DOS, we found that the assumption of a separate finite background DOS (c) is necessary for producing good fits to experimental data. The presence of a significant background DOS is a further manifestation of a strong inverse proximity effect, a signature of which is the deviation from conventional BCS DOS, in the form of producing strong background DOS [24,25]. Within the large error bars, the value of c appears approximately independent of field, but more experimental work is

required for unambiguous confirmation of the effect. We note that there are suggestions regarding the existence of FFLO phase leading to such a background DOS [26], however this cannot be confirmed in our experiment.

In conclusion, this work confirms the presence of interfacial exchange fields at S/FI interfaces even though the thickness of the S layer is far greater than its coherence length. Unlike previous studies of Al, the exchange field in NbN is found to remain constant over the entire applied magnetic field range as demonstrated via two independent methods to derive the magnitude of internal exchange field. Because of the strongly spin-filtering nature of the barrier the exchange field can be extracted from the conductance curves without fitting them. Nevertheless we can accurately fit the spectra and the fits suggest a strong inverse proximity effect in addition to the exchange field. It is worth noting here that in S/FI/S Josephson junctions with identical FI thickness, we have observed pure second harmonic current phase relation [13], which indicated unconventional superconductivity and so there is the potential for intrinsic exchange fields or inverse proximity effects in NbN layer to be the origin of unconventional superconducting correlations. The confirmation of the interfacial nature of the exchange field makes GdN a suitable ferromagnetic insulating material that could be used in conjunction with s-wave superconductors and topological insulators for carrying out proposed experiments aimed at creation and detection of Majorana bound states [27,28].

This work was supported by the ERC Advanced Investigator Grant (Superspin).

*ap638@cam.ac.uk

-
- [1] R. Meservey, P. M. Tedrow, and P. Fulde, Phys. Rev. Lett. **25**, 1270 (1970).
 - [2] P. M. Tedrow and R. Meservey, Phys. Rev. Lett. **26**, 192 (1971).
 - [3] A. Larkin and A. Ovchinnikov, Sov. Phys. JETP **20**, 762 (1965).
 - [4] P. Fulde and R. A. Ferrell, Phys. Rev. **135**, A550 (1964).
 - [5] F. Bergeret, A. Yeyati, and A. Martín-Rodero, Phys. Rev. B **72**, 064524 (2005).
 - [6] J. Xia, V. Shelukhin, M. Karpovski, A. Kapitulnik, and A. Palevski, Phys. Rev. Lett. **102**, 087004 (2009).
 - [7] P. G. de Gennes, Physics Letters **23**, 10 (1966).
 - [8] P. M. Tedrow, J. E. Tkaczyk, and A. Kumar, Phys. Rev. Lett. **56**, 1746 (1986).
 - [9] J. S. Moodera, X. Hao, G. A. Gibson, and R. Meservey, Phys. Rev. Lett. **61**, 637 (1988).
 - [10] X. Hao, J. S. Moodera, and R. Meservey, Phys. Rev. B **42**, 8235 (1990).

- [11] X. Hao, J. S. Moodera, and R. Meservey, Phys. Rev. Lett. **67**, 1342 (1991).
- [12] A. Pal, K. Senapati, Z. H. Barber, and M. G. Blamire, Adv. Mater. **25**, 5581 (2013).
- [13] A. Pal, Z. H. Barber, J. W. A. Robinson, and M. G. Blamire, Nature Commun. **5**, 3340 (2014).
- [14] M. G. Blamire, A. Pal, Z. H. Barber, and K. Senapati, SPIE 2012 **8463**, 84610J (2012).
- [15] R. C. Dynes, V. Narayanamurti, and J. P. Garno, Phys. Rev. Lett. **41**, 1509 (1978).
- [16] E. S. Sadki, Z. H. Barber, S. J. Lloyd, M. G. Blamire, and A. M. Campbell, Phys. Rev. Lett. **85**, 4168 (2000).
- [17] B. S. Chandrasekhar, Appl. Phys. Lett. **1**, 7 (1962).
- [18] A. M. Clogston, Phys. Rev. Lett. **9**, 266 (1962).
- [19] T. Penney, M. W. Shafer, and J. B. Torrance, Phys. Rev. B **5**, 3669 (1972).
- [20] Y. M. Xiong, S. Stadler, P. W. Adams, and G. Catelani, Phys. Rev. Lett. **106**, 247001 (2011).
- [21] R. Meservey, P. M. Tedrow, and R. C. Bruno, Phys. Rev. B **11**, 4224 (1975).
- [22] K. Maki, Progress of Theoretical Physics **31**, 731 (1964).
- [23] M. Šindler, *et al.*, SUST **27**, 055009 (2014).
- [24] M. A. Sillanpää, T. T. Heikkilä, R. K. Lindell, and P. J. Hakonen, EPL **56**, 590 (2001).
- [25] A. Cottet and J. Linder, Phys. Rev. B **79**, 054518 (2009).
- [26] Y. L. Loh, N. Trivedi, Y. M. Xiong, P. W. Adams, and G. Catelani, Phys. Rev. Lett. **107**, 067003 (2011).
- [27] L. Fu and C. L. Kane, Phys. Rev. Lett. **100** (2008).
- [28] L. Fu and C. L. Kane, Phys. Rev. Lett. **102** (2009).

Y. Naidyuk, H. Löhneysen, and I. Yanson, Phys. Rev. B **54**, 16077 (1996).